Cell Reports, Volume *30*

Supplemental Information

Vitamin B12 Regulates Glial Migration and Synapse Formation through Isoform-Specific Control of PTP-3/LAR PRTP Expression

Albert Zhang, Brian D. Ackley, and Dong Yan

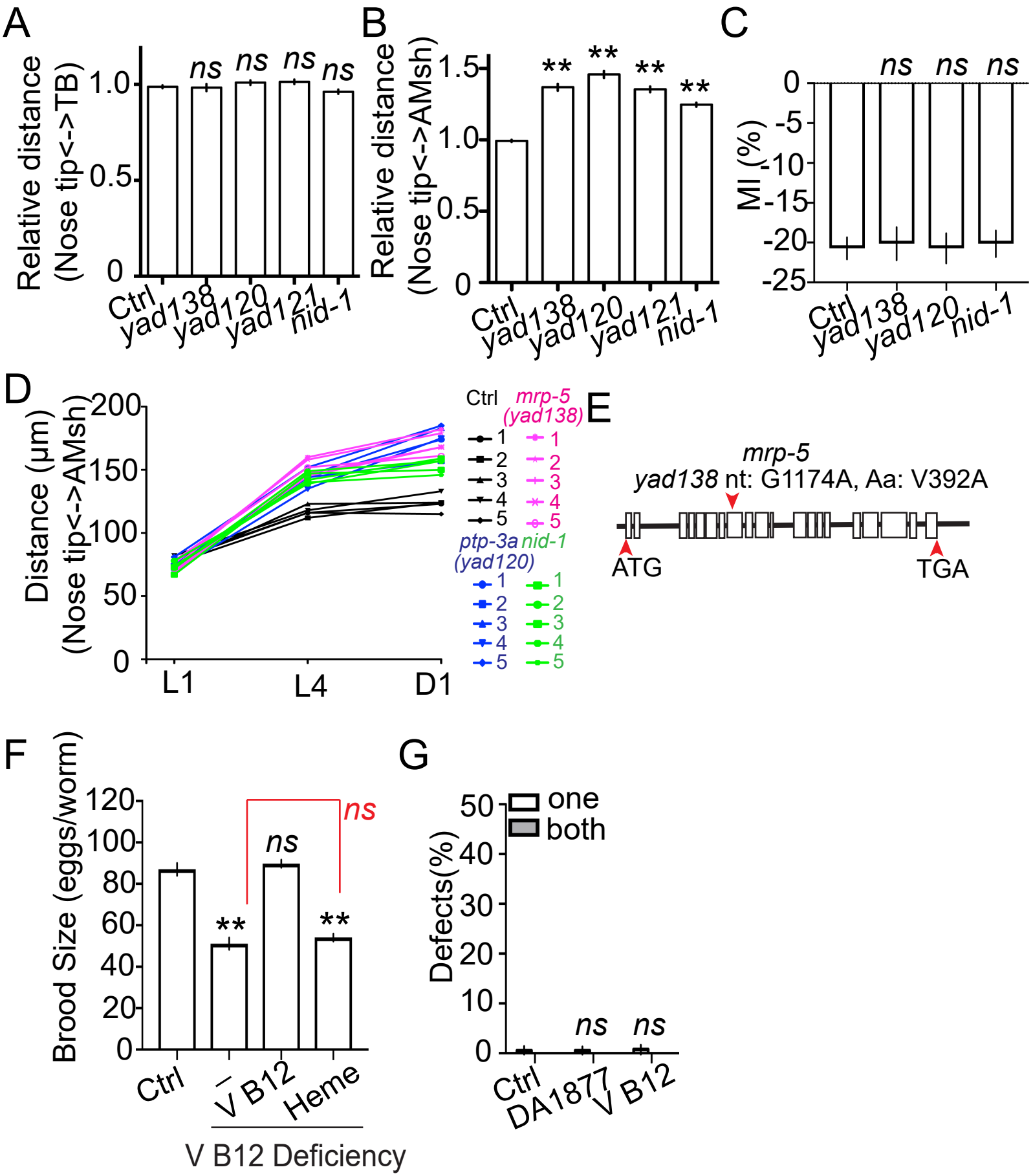

Supplemental Figure 1, Vitamin B12 is critical for AMsh glial migration.
Related to Figures 1, 2 and 4.

(**A**) Data showing the relative distance between the nose tip and the center of the pharyngeal terminal bulb (TB) in control and mutant D1 animals. Data are normalized by the average distance between the nose tip and the center of the TB in control animals.

(**B**) Data showing the relative distance between the nose tip and the center of AMsh cell bodies in control and mutant D1 animals. Data are normalized by the average distance between the nose tip and the center of the AMsh cell bodies in control animals.

(**C**) Data showing the Migration Index of control and mutant animals at the L1 stage.
(**D**) Data showing the distance between the nose tip and the center of AMsh cell bodies at different developmental stages of individual animals. Five animals were quantified for each genotype, and each animal is represented by a single line.
(**E**) *yad138* caused a missense mutation in *mrp-5*.
(**F**) Data showing the brood size of animals grown in vitamin B12-deficient conditions for five generations with/without vitamin B12 or heme supplementation.
(**G**) Data showing the percentage of animals with AMsh migration defects when fed a vitamin B12 enriched diet either by feeding the *E. coli* DA1977 strain or directly adding 100 μg/L vitamin B12.
In Figs. **A**, **B**, **C**, and **F**, data are represented as mean ± SEM. One-way ANOVA test. **, $P<0.01$; ns, no significant difference. Each point represents at least 20 worms. In Fig. **G**, data are represented as mean ± SEM. Two-way ANOVA test. **, $P<0.01$; ns, no significant difference. Each point represents three experiments of at least 50 worms.

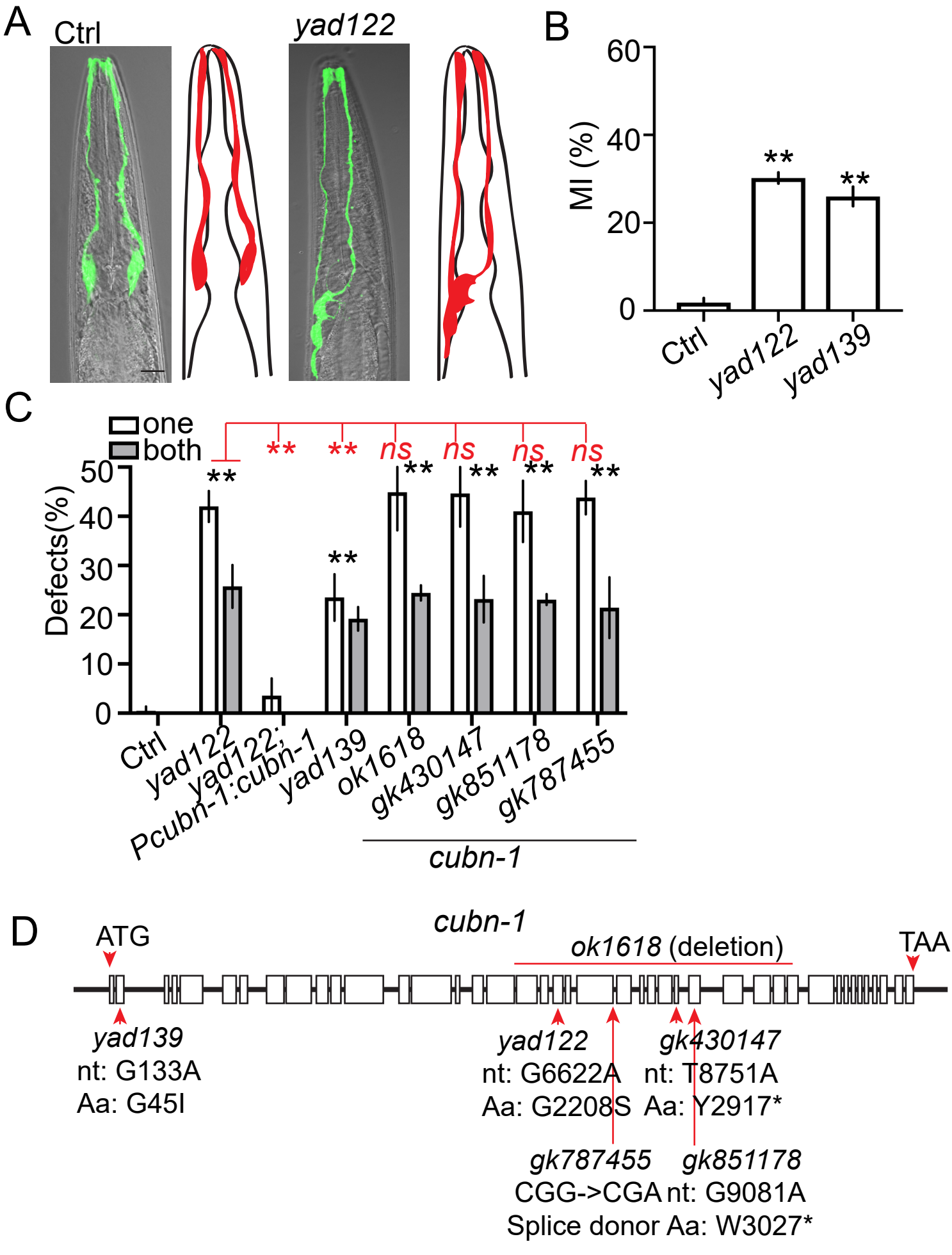
A
Ctrl
yad122
B
MI (%)
60
40
20
0
**
**
Ctrl
yad122
yad139
C
one
both
**
**
ns
ns
ns
ns
Defects(%)
50
40
30
20
10
0
**
**
**
**
**
Ctrl
yad122
yad122;
Pcubn-1:cubn-1
yad139
ok1618
gk430147
gk851178
gk787455
cubn-1
D
cubn-1
ATG
ok1618 (deletion)
TAA
yad139
nt: G133A
Aa: G45I
yad122
nt: G6622A
Aa: G2208S
gk430147
nt: T8751A
Aa: Y2917*
gk787455
CGG->CGA
Splice donor
gk851178
nt: G9081A
Aa: W3027*

Supplemental Figure 2, *cubn-1* functions in AMsh glial cells to terminate migration.
Related to Figure 1.

(**A**) *yad122* causes over-migration of AMsh glia. Confocal images and schematic representation of AMsh glia in control and *cubn-1(yad122)* animals expressing *Pf53f4.13::GFP (yadIs48)*. TB: pharyngeal terminal bulb. Scale bar, 10 μm.

(**B**) Quantification of Migration Index (MI) in control, *cubn-1(yad122)*, and *cubn-1 (yad138)* animals. MI is calculated as described in Fig. 1**B**.

(**C**) *yad122* is a null allele of *cubn-1*. White and grey bars show the percentage of animals with over-migration defects in one AMsh or both AMsh glia respectively. *ok1618*, *gk430147*, *gk851178*, *gk787455* are predicted null alleles of *cubn-1*.

(**D**) *yad122* and *yad139* caused missense mutations in *cubn-1*. *ok1618*, *gk430147*, *gk787455* and *gk851178* all caused premature stop codons.

In Fig. **B**, data are represented as mean ± SEM. One-way ANOVA test. **, P<0.01; Each point represents at least 30 worms. In Fig. **C**, data are represented as mean ± SEM. Two-way ANOVA test. **, P<0.01; ns, no significant difference. Each point represents three experiments of at least 50 worms each.

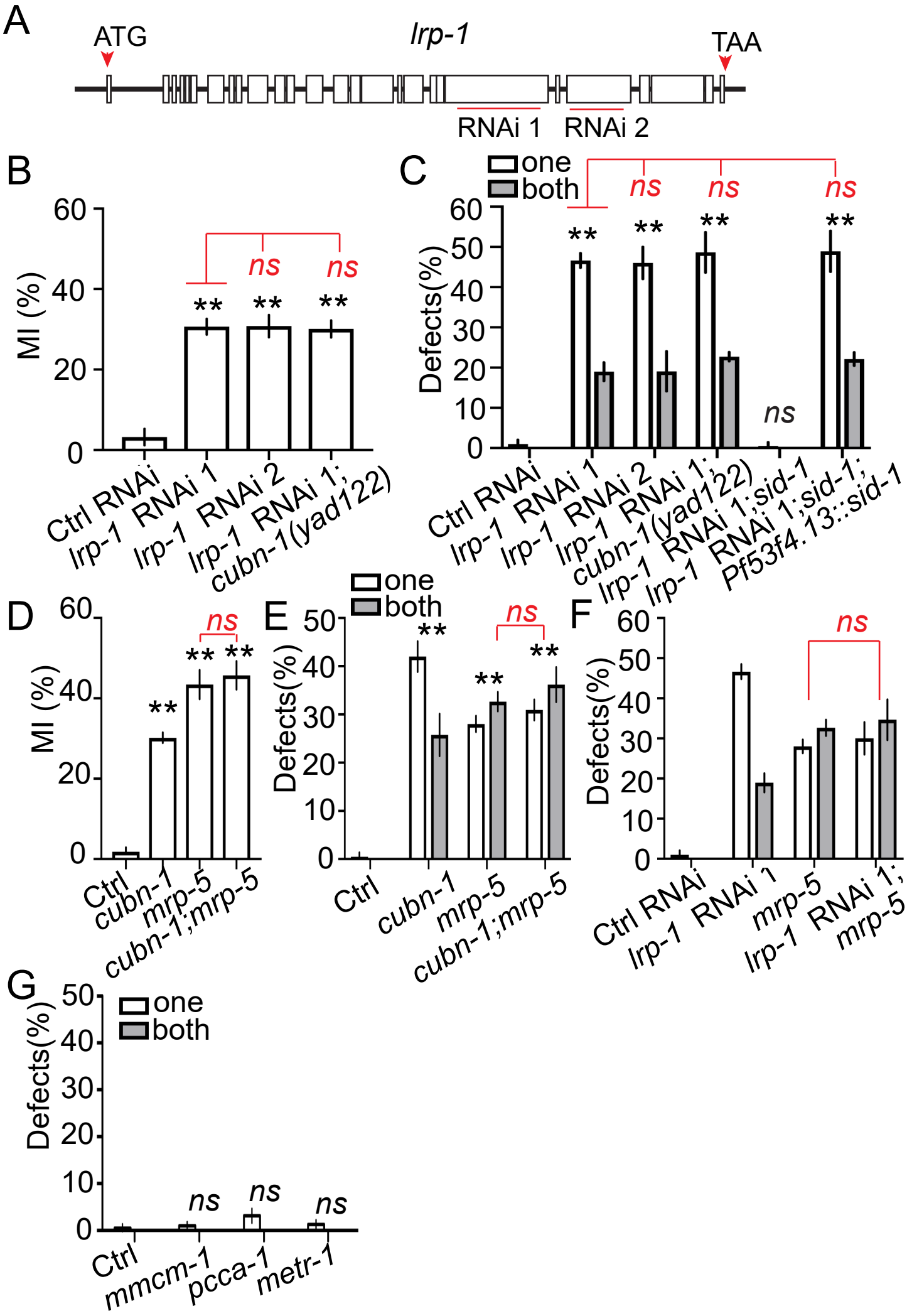
A
ATG
lrp-1
TAA
RNAi 1
RNAi 2
B
MI (%)
ns
ns
**
**
**
Ctrl RNAi
lrp-1 RNAi 1
lrp-1 RNAi 2
lrp-1 RNAi 1; cubn-1(yad122)
C
one
both
Defects(%)
ns
ns
ns
**
**
**
**
ns
Ctrl RNAi
lrp-1 RNAi 1
lrp-1 RNAi 2
lrp-1 RNAi 1; cubn-1(yad122)
lrp-1 RNAi 1;sid-1
lrp-1 RNAi 1;sid-1; Pf53f4.13::sid-1
D
MI (%)
ns
**
**
**
Ctrl
cubn-1
mrp-5
cubn-1;mrp-5
E
one
both
Defects(%)
ns
**
**
**
Ctrl
cubn-1
mrp-5
cubn-1;mrp-5
F
Defects(%)
ns
Ctrl RNAi
lrp-1 RNAi 1
mrp-5
lrp-1 RNAi 1; mrp-5
G
one
both
Defects(%)
ns
ns
ns
Ctrl
mmcm-1
pcca-1
metr-1

Supplemental Figure 3, *cubn-1* and *lrp-1* are required for AMsh glial migration.
Related to Figure 1.
(**A**) The positions of two *lrp-1* RNAi probes.
(**B-C**) *lrp-1* cell autonomously regulates AMsh migration. Global knockdown and AMsh specific knockdown of *lrp-1* cause similar AMsh over migration defects and did not further enhance *cubn-1(lf)* phenotypes (**B**, Migration Index; **C**, percentage of animals with migration defects).
(**D-E**) (**D**) Quantification of Migration Index (MI) and (**E**) percentage of animals with AMsh migration defects in *cubn-1;mrp-5* double mutants.
(**F**) Knockdown of *lrp-1* does not enhance *mrp-5(lf)* phenotypes.
(**G**) Data show the percentage of animals with AMsh migration defects in *mmcm-1*, *pcca-1*, and *metr-1* mutants.
In Figs. **B** and **D**, data are represented as mean ± SEM. One-way ANOVA test. **, P<0.01; Each point represents at least 30 worms. In Figs. **C**, **E**, **F** and **G**, data are represented as mean ± SEM. Two-way ANOVA test. **, P<0.01; ns, no significant difference. Each point represents three experiments of at least 50 worms.

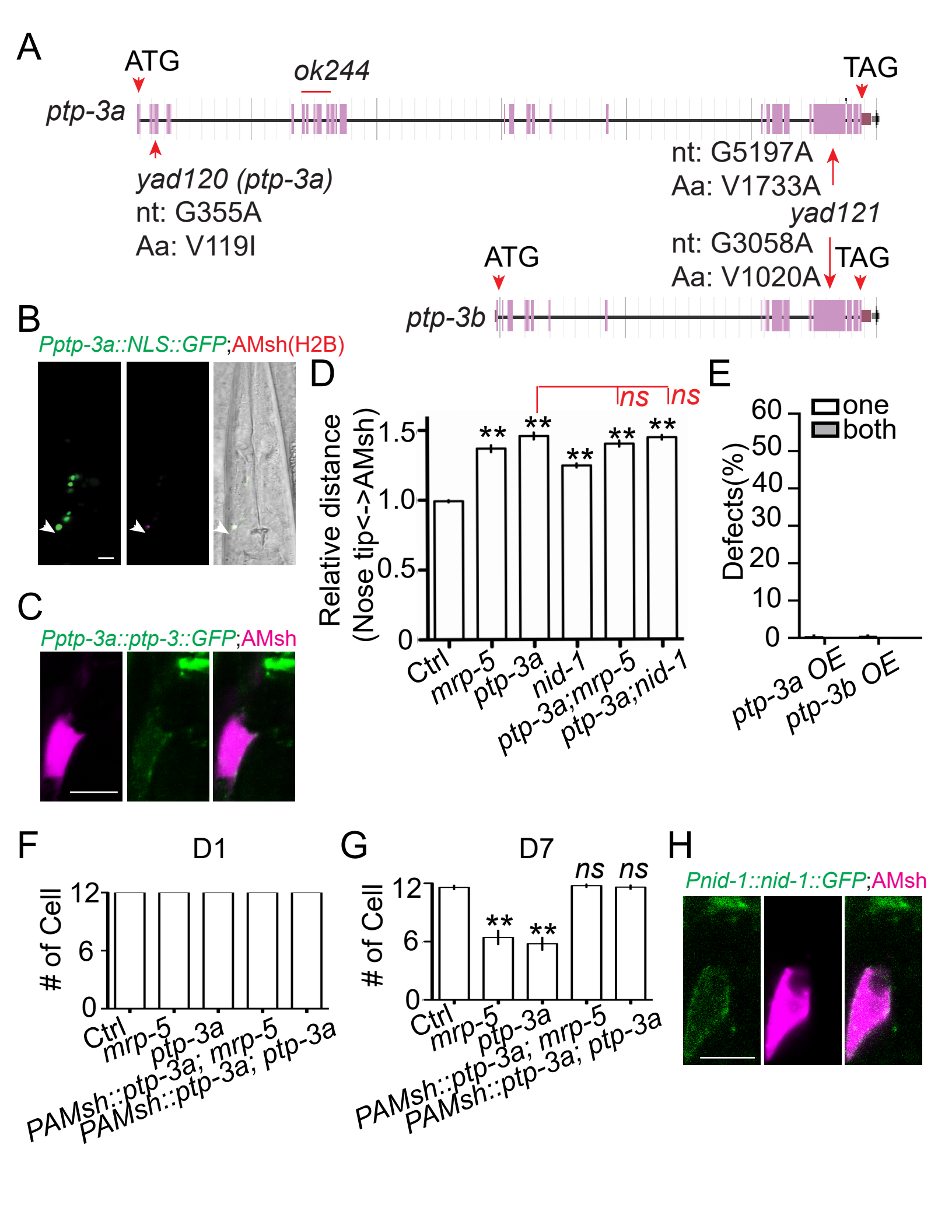
A
ATG
ok244
TAG
ptp-3a
yad120 (ptp-3a)
nt: G355A
Aa: V119I
nt: G5197A
Aa: V1733A
yad121
nt: G3058A
Aa: V1020A
ATG
TAG
ptp-3b
B
Pptp-3a::NLS::GFP;AMsh(H2B)
C
Pptp-3a::ptp-3::GFP;AMsh
D
Relative distance (Nose tip<->AMsh)
ns
ns
**
Ctrl
mrp-5
ptp-3a
nid-1
ptp-3a;mrp-5
ptp-3a;nid-1
E
Defects(%)
one
both
ptp-3a OE
ptp-3b OE
F
D1
# of Cell
Ctrl
mrp-5
ptp-3a
PAMsh::ptp-3a; mrp-5
PAMsh::ptp-3a; ptp-3a
G
D7
ns
ns
**
H
Pnid-1::nid-1::GFP;AMsh

Supplemental Figure 4, *ptp-3a* and *nid-1* regulates AMsh glial migration.
Related to Figures 2, 3 and 4.

(**A**) *yad120* causes a missense mutation in *ptp-3a*, and *yad121* causes a missense mutation in both *ptp-3a* and *ptp-3b*.

(**B-C**) Single plane confocal images show *ptp-3a* is expressed in AMsh cells. (**B**) GFP signal (left panel) shows expression of nuclear-localized GFP driven by the *ptp-3a* promoter. mCherry signal (middle panel) is from expression of mCherry::H2B under an AMsh-specific promoter (*Pf53f4.13*). The right panel shows a merged image of DIC, GFP and mCherry signal. (**C**) mCherry signal (left) shows expression of free mCherry under an AMsh-specific promoter (*Pf53f4.13*). GFP signal (middle panel) shows expression of PTP-3A::GFP driven by the *ptp-3a* promoter. Scale bar, 10 μm.

(**D**) Data showing the relative distance between the nose tip and the center of the AMsh cell bodies in control and mutant animals. Data are normalized by the average distance between the nose tip and the center of the AMsh cell bodies in control animals.

(**E**) Data showing the percentage of animals with AMsh migration defects for different genotypes.

(**F-G**) The number of neurons visualized by DiI in D1 (**F**) and D7 (**G**) animals.

(**H**) GFP signal (left panel) shows expression of NID-1::GFP driven by the *nid-1* promoter. mCherry signal (middle panel) is from expression of mCherry::H2B under an AMsh-specific promoter (*Pf53f4.13*). The right panel shows a merged image of GFP and mCherry signal. All images are from single focal planes. Scale bar, 10 μm.

In Figs. **D**, **F** and **G** data are represented as mean ± SEM. One-way ANOVA test. **, $P<0.01$; ns, no significant difference. Each point represents at least 20 worms. In Fig. **E**, data are represented as mean ± SEM. Two-way ANOVA test. **, $P<0.01$; ns, no significant difference. Each point represents three experiments of at least 50 worms.

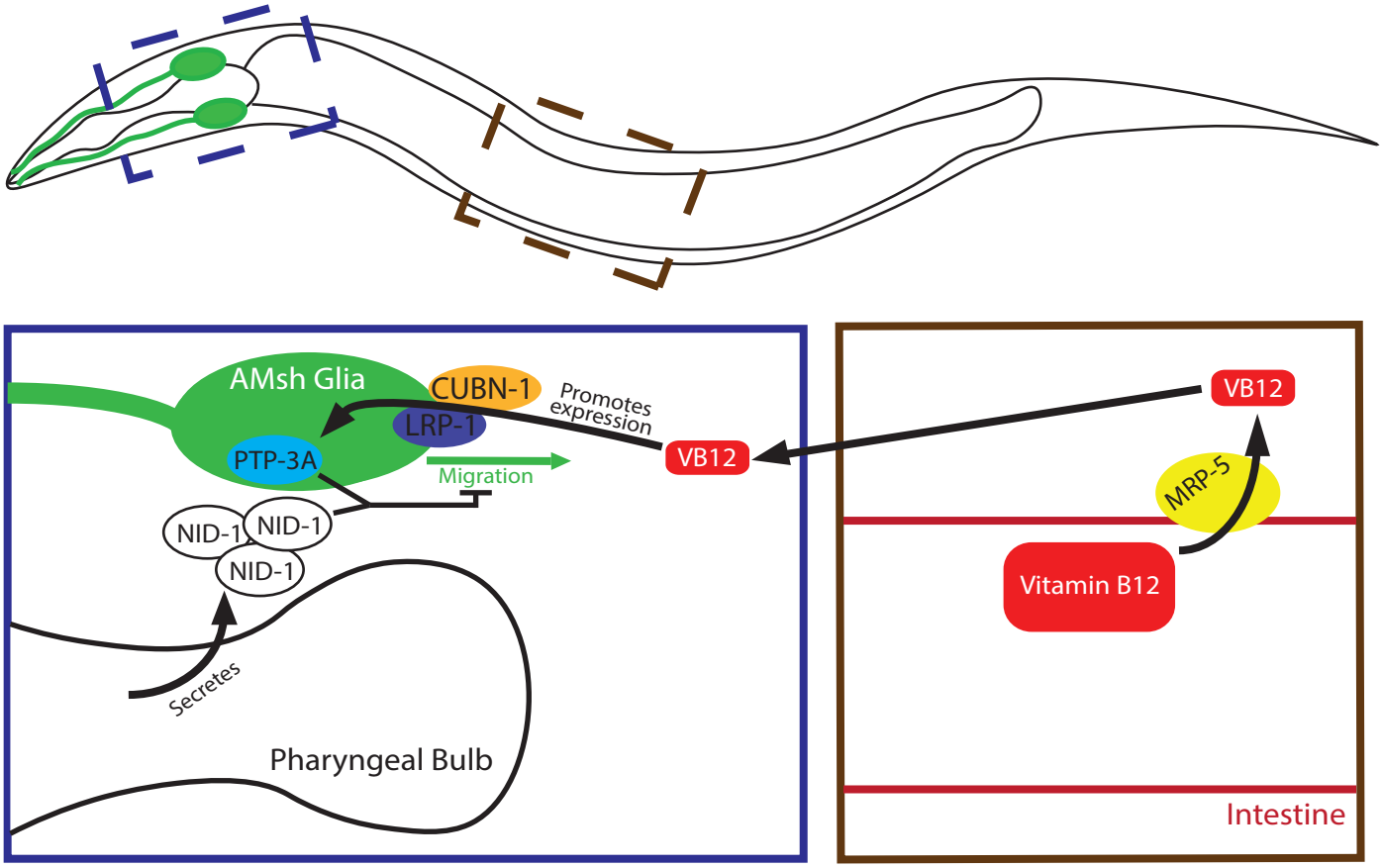

Supplemental Figure 5, A model for regulation of AMsh glial migration by vitamin B12. Related to Figures 1, 2, 3 and 4.